Talanta 93 (2012) 345–349

Contents lists available at SciVerse ScienceDirect

Talanta

journal homepage: www.elsevier.com/locate/talanta

One-step synthesis of graphene–AuNPs by HMTA and the electrocatalytical application for O_2 and H_2O_2

Jianguo Hu[a,b], Fenghua Li[a], Kaikai Wang[a], Dongxue Han[a], Qixian Zhang[a,*], Junhua Yuan[b,*], Li Niu[a]

[a] Engineering Laboratory for Modern Analytical Techniques, c/o State Key Laboratory of Electroanalytical Chemistry, Changchun Institute of Applied Chemistry, Chinese Academy of Sciences, Changchun 130022, PR China
[b] Laboratory of Biomimetic Electrochemistry and Biosensors, Department of Chemistry and Life Sciences, Zhejiang Normal University, Jinhua 321004, PR China

ARTICLE INFO

Article history:
Received 8 December 2011
Received in revised form 20 February 2012
Accepted 22 February 2012
Available online 1 March 2012

Keywords:
Graphene
AuNPs
HMTA
One-step method
Electrocatalytic activity

ABSTRACT

A green, one-step method for synthesis of graphene–Au nanoparticles (graphene–AuNPs) was introduced in this article, using an environmentally benign hexamethylenetetramine (HMTA) as reducing and stabilizing agent. HMTA slowly was hydrolyzed to generate aldehyde ammonia to reduce graphene oxides (GO) and hydrogen tetrachloroaurate (Au precursor). The structure and composition of the graphene–AuNPs nanocomposites were studied by means of ultraviolet visible (UV) absorption spectra, X-ray photoelectron spectroscopy (XPS) and Transmission electron microscopy (TEM). The AuNPs are well-dispersed on graphene nanosheets in narrow size range. The nanocomposites have excellent electrocatalytical properties for catalytic reduction of O_2 and H_2O_2.

1. Introduction

Graphene, a two dimensional monoatomic thick building block of a carbon allotrope, has triggered extensive attention in electrochemical studies, due to its fascinating electronic and mechanical properties [1,2], since its discovery by Geim and co-workers in 2004 [3]. Because of its unique nanostructure and extraordinary properties, graphene is not only a basic building block for graphitic materials of all other dimensionalities [1], but also considered to be the thinnest and strongest materials [4]. However, pure graphene cannot remain good dispersibility as single-layer sheets in aqueous solution [5,6]. To overcome this problem, the functionalization of graphene has been considered to be an important method for expanding its application in recent years [7]. In addition, graphene-based nanocomposites have been received increased attention due to the synergistic contribution of two or more functional components and its many potential applications [8,9]. Up to now, a number of works have reported for graphene–metal nanocomposites, such as Au [10–17], Ag [16], Pt [17], and Pd [18] decorated graphene nanosheets.

As well known, Au nanoparticles (AuNPs) are one of the most intensively studied and applied metal nanoparticles in electrochemistry due to their extraordinarily physical and chemical properties [19–21]. These unique properties allow them to provide major functions like electroanalysis and construct electrochemical sensors [22,23]. Herein, AuNPs are decorated on graphene nanosheets to enhance the electrocatalytic activity of the nanocomposites by improving their electrical conductivity. However, the electrocatalytic activity of graphene–AuNPs nanocomposites greatly depends on the size and dispersion of the AuNPs. Therefore, the method of synthesizing AuNPs in narrow size and good dispersion requires for further study. Different synthetic methods have been developed to prepare the desired AuNPs. One of the common methods is the reduction of hydrogen tetrachloroaurate (Au precursor) by sodium citrate [24]. AuNPs synthesized by such method are in big size. In the Brust method, AuNPs were reduced by sodium borohydride in the presence of alkylthiols [25], but the disadvantage of this method introduces the contamination of boride impurities. A few other one-step reduction processes were also developed to generate monodispersed AuNPs [26,27], for example, some amine-containing organic reagent can reduce Au precursor to AuNPs [28–30]. This method is limited to organic media.

Hexamethylenetetramine (HMTA), a heterocyclic organic compound with cage-like structure similar to adamantine as an environmentally friendly reagent, is widely applied in aqueous-phase synthesis. Owing to its inexpensiveness, commercial availability, high solubility in water and polar organic solvents, HMTA has been applied in a broad variety of fields [31]. It can serve as a reductant to prepare water-soluble metal nanoparticles [32], in which metal precursor is reduced in situ by the generated

* Corresponding authors. Fax: +86 431 8526 2800.
E-mail addresses: qxzhang@ciac.jl.cn (Q. Zhang), jhyuan@zjnu.cn (J. Yuan).

0039-9140/$ – see front matter © 2012 Published by Elsevier B.V.
doi:10.1016/j.talanta.2012.02.050

aldehyde ammonia from the hydrolysis of HMTA in water [32–34]. Recently, HMTA was also used as an effective reductant to prepare graphene nanosheets with highly stable aqueous colloidal dispersions [35]. So it is possible that HMTA can act as an effective reducer and stabilizer to simultaneously reduce the Au precursor and graphene oxides (GO) to produce the graphene–AuNPs nanocomposites under mild conditions.

In this paper, one-step method was firstly adopted to synthesize the graphene–AuNPs nanocomposites from GO and Au precursor with the help of HMTA. HMTA was able to ensure the homogeneous nucleation of AuNPs at the initial process by slowing the reaction rate. HMTA was slowly hydrolyzed to generate aldehyde ammonia, which could reduce Au precursor and GO to form well-dispersible AuNPs decorated graphene nanosheets. The attachment of AuNPs onto graphene not only prevents the restack of these sheets during the chemical reduction process, but also leads to the formation of a new class of graphene-based nanocomposites. The nanocomposites modified glassy carbon electrode (graphene–AuNPs/GCE) shows excellent electrocatalytic activity toward O_2 and H_2O_2. The good electrocatalytic activity provides greatly importance to its potential application in chemical sensors and biosensors.

2. Experimental

2.1. Reagents and materials

Graphite powders (320 mesh) were of spectroscopic purity and purchased from Shanghai Chemicals, China. $HAuCl_4{\cdot}3H_2O$ was obtained from Aldrich. Hydrogen peroxide solution (30 wt% aqua) was purchased from Beijing Chemicals. Hexamethylenetetramine and sodium oleate were both purchased from Shanghai Chemical Reagent Company and used without further purification. Unless otherwise stated, reagents were of analytical grade and used as received. Aqueous solutions were prepared with double-distilled water from a Millipore system (>18 MΩ cm).

2.2. Instruments

Ultraviolet visible (UV) absorption spectra were recorded by a Hitachi U-3900 spectrometer. Transmission electron microscopy (TEM) images were obtained using a Hitachi-600 transmission electron microscope operating at 100 kV. X-ray photoelectron spectroscopy (XPS) analysis was carried out on an ESCALAB MK II X-ray photoelectron spectrometer. Cyclic voltammetry (CV) measurements were carried out using a conventional three-electrode system with a platinum wire as auxiliary electrode and an Ag/AgCl (3 M KCl) as reference electrode in a CHI 660A Electrochemical Workstation (CHI, USA). The working electrodes were bare or modified (GCE, d: 3 mm). Before utilization, GCE was carefully polished to a mirror finish with 1.0, 0.3 and 0.05 nm alumina slurries successively, and rinsed with double-distilled water, followed by sonication in acetone and double-distilled water in succession, and finally dried in N_2. The electrolyte solution used for CV experiment was 0.05 M phosphate buffer solution (PBS, pH 7.4), which was used in all electrochemical studies unless otherwise stated.

2.3. Synthesis of GO

GO was synthesized from natural graphite powder by a modified Hummers method [36,37]. The graphite powder (10 g) was put into an 80 °C solution of concentrated H_2SO_4 (15 mL), $K_2S_2O_8$ (5 g), and P_2O_5 (5 g). The mixture was kept at 80 °C for 4.5 h using a hotplate. Successively, the mixture was cooled to room temperature, and diluted with distilled water, filtered, and washed on the filter until the rinse water pH became neutral. The preoxidized graphite was dried in air at ambient temperature. The oxidized graphite powder (10 g) was put into cold (0 °C) concentrated H_2SO_4 (230 mL). Then, $KMnO_4$ (30 g) was added gradually under stirring and the temperature of the mixture was kept to be below 20 °C by cooling. The mixture was then stirred at 35 °C for 2 h, and distilled with distilled water (460 mL). The temperature of the mixture increased to 98 °C and maintained for 15 min. The reaction was terminated by the addition of a large amount of distilled water (1.4 L) and 30% H_2O_2 solution (25 mL). The mixture was filtered and washed with 1:10 HCl solution (2.5 L) in order to remove metal ions. The GO dispersion was subjected to dialysis 3–4 days to completely remove metal ions and acids. Finally, the resulting purified GO powders were collected by centrifugation and air drying.

2.4. Synthesis of graphene and graphene–AuNPs nanocomposites

A general procedure for the preparation of graphene–AuNPs nanocomposites is described as follows. At first, 0.015 g $HAuCl_4{\cdot}3H_2O$ were dissolved in 1.25 mL of 0.1 M HCl solution and 0.0125 g sodium oleate were dissolved in 10.0 mL of double distilled water under stirring, respectively. Then the above two solutions were mixed to be a lemon solution. The resulting solution was dropwisely added to 10 mL GO in a 50 mL round-bottom flask. Next, 0.15 g HMTA were mixed under vigorous stirring for 10 min, and in this process, the pH of this mixture was adjusted to 13.0 with addition of 0.4 M KOH. Subsequently, the mixture was refluxed in an oil bath at 80 °C under stirring for 80 min over which the color of the solution gradually changed into amaranth. Finally, the resulting nanocomposites were centrifuged and collected for 12 min at 8000 rpm. HMTA could be hydrolyzed in aqueous solution generating ammonia and formaldehyde little by little, which reduces Au precursor to uniformly dispersed AuNPs decorating graphene nanosheets. In this procedure, in order to control the growth and size of the final produced AuNPs, sodium oleate was regarded as the surfactant. Uniform vesicle structures could be generated in aqueous systems. In this process, when water-soluble Au precursor was dispersed in the sodium oleate solution, many separated micro-reactors were formed for the synthesis of well-dispersed AuNPs. As a result, GO and Au precursor could be reduced to the narrow size and favorable dispersion of graphene–AuNPs nanocomposites. Scheme 1 shows the chemical structure of HMTA and the schematic of the process for preparing the graphene–AuNPs nanocomposites. The graphene was prepared according to a previous report [35].

2.5. Fabrication of graphene/GCE and graphene–AuNPs/GCE nanocomposites films

The GCEs were polished subsequently with 1.0, 0.3 and 0.05 μm alumina slurry, and then sonicated in water for several times. To prepare graphene and graphene–AuNPs modified GCE, an aliquot of 5 μL 2.5 mg mL^{-1} graphene and graphene–AuNPs aqueous solution was dropped onto the surface of GCE using a microsyringe, respectively. The dried films could be obtained after 10 h at 4 °C.

3. Results and discussion

3.1. Structure characterization

The UV absorption spectra, XPS and TEM studies were carried out to investigate the chemical and structural information of the as-prepared graphene–AuNPs nanocomposites. The UV absorption spectra of GO (black), the reduced GO (blue) and graphene–AuNPs aqueous solutions (red) were shown in Fig. S1. The UV absorption spectra of the GO dispersion reached an absorption peak at ca. 227 nm (curve a in Fig. S1). When the GO aqueous dispersion was reduced by HMTA, the absorption peak red shifts to 254 nm (curve

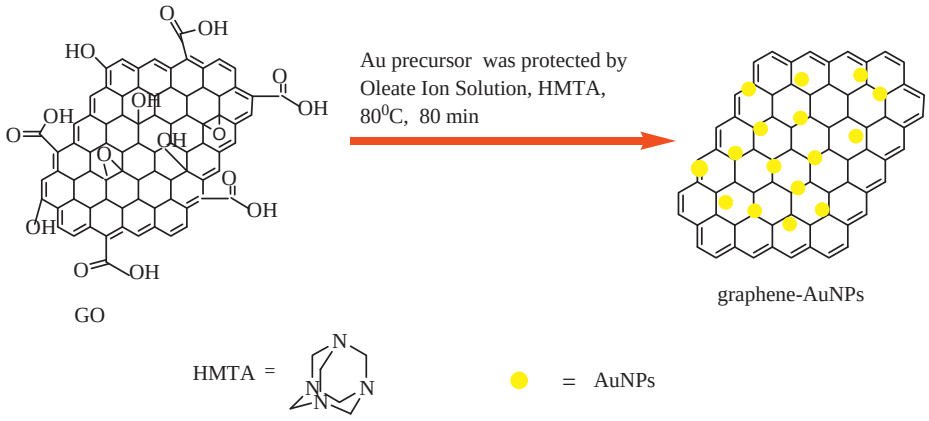

Scheme 1. Synthesis of the graphene–AuNPs nanocomposites.

b in Fig. S1), suggesting that the electronic conjugation within graphene nanosheets had been restored after the reaction. However, when AuNPs were decorated onto the graphene nanosheets, two absorption peaks of graphene–AuNPs nanocomposites were observed at 253 and 532 nm (curve c in Fig. S1), which were corresponding to the absorption of graphene and AuNPs, respectively. Meanwhile, the inset photograph displays that the color of the solution turning from pale brown to black further confirming the reduction process.

The nanocomposites of the graphene–AuNPs were further confirmed by the XPS results in Fig. 1(A). The nanocomposites showed an obvious C1s peak at 284.6 eV (carbon in C—C) and O1s peak at 532.0 eV, which also exhibited unobvious Au4f peak (top-right inset). The top right inset represented the XPS signature of the Au4f doublet ($4f_{7/2}$ and $4f_{5/2}$) of the resulting AuNPs. The Au $4f_{7/2}$ and Au $4f_{5/2}$ peaks appeared at ca. 83.7 and 87.3 eV (peak-to-peak distance of 3.6 eV), respectively, which were consistent with previous report confirming the formation of metallic gold [38].

The C1s XPS spectra of GO and graphene–AuNPs nanocomposites were shown in Fig. 1(B) and (C), respectively. Although the C1s XPS spectrum of the graphene–AuNPs showed the same four components corresponding to carbon atoms in oxygen functionalities with GO. The absorption peaks of graphene at 286.6 eV (carbon in C—O), 287.9 eV (carbonyl carbon) and 288.90 eV (carboxylate carbon) were sharply decreased, indicating the deoxygenation process. The interaction between graphene nanosheets and AuNPs was confirmed.

Fig. 2 displays the TEM images of graphene nanosheets and graphene–AuNPs nanocomposites. As shown in Fig. 2(A), the TEM image of graphene nanosheets illustrated the flake-like shapes of graphene. In Fig. 2(B), the graphene nanosheets have been decorated by AuNPs, and the AuNPs covered the most part of the surface of the graphene nanosheets in fairly even, non-ordered distribution. Moreover, a narrow size-distribution histogram was also obtained from measuring 100 randomly selected nanoparticles (inset of Fig. 2(B)). Very few of AuNPs did not count to the histogram, because of the size over 10 nm. The diameter of AuNPs ranges from 2 to 7 nm, with a mean diameter of 4 nm, and the AuNPs dispersed very uniformly. The absence of isolated AuNPs in the product indicated that the interaction between the particles and graphene was strong.

3.2. *Electrocatalysis of H_2O_2 and O_2 at graphene–AuNPs/GCE*

The graphene–AuNPs/GCE exhibited a high electrocatalytic activity towards the reduction of H_2O_2. Fig. 3 shows the electrocatalytic reduction of H_2O_2 at bare GCE, graphene/GCE, and graphene–AuNPs/GCE, respectively. We compared the electrocatalysis towards H_2O_2 at the graphene–AuNPs/GCE in N_2-saturated PBS solution (black), the bare GCE in the presence of 0.05 M H_2O_2 in N_2-saturated PBS solution (red), the graphene/GCE in the presence of 0.05 M H_2O_2 in N_2-saturated PBS solution (blue), and the graphene–AuNPs/GCE in the presence of 0.05 M H_2O_2 in N_2-saturated PBS solution (green). The bare GCE showed hardly catalytic effect towards H_2O_2 reduction, and the response current of graphene/GCE was very small. However, the more obvious catalytic current and earlier onset potentials in the process of reduction at graphene–AuNPs/GCE were observed, due to the synergistic effect

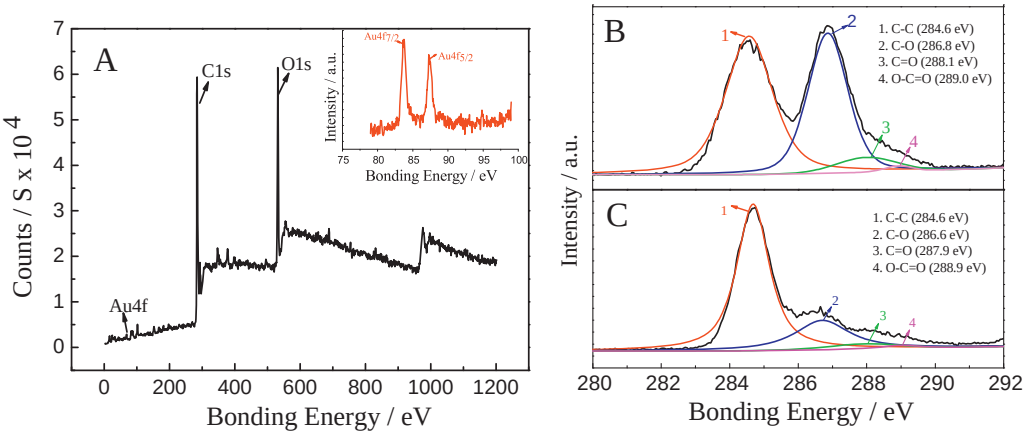

Fig. 1. XPS spectra of the graphene–AuNPs nanocomposites (A), insets: the Au4f doublet; the C1s XPS spectra of the GO (B) and graphene–AuNPs nanocomposites (C).

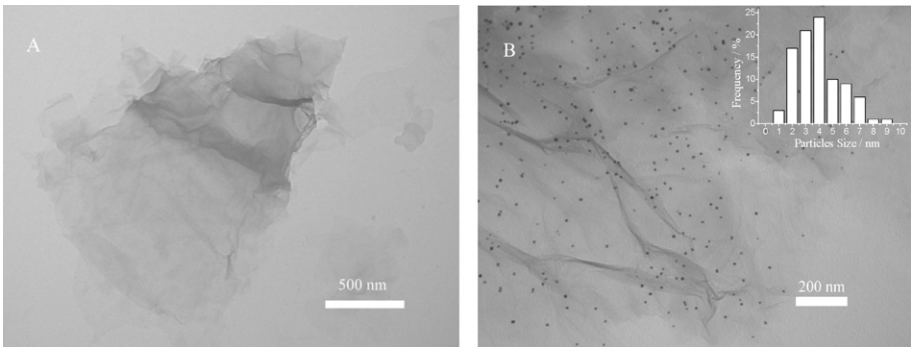

Fig. 2. TEM images of the graphene nanosheets (A) and graphene–AuNPs nanocompoites (B). Inset: the particle size distribution histogram of the AuNPs obtained from measuring 100 randomly selected nanoparticles.

of graphene and AuNPs, which indicated that the nanocomposites have much better electrocatalytic activity toward the reduction of H_2O_2.

Fig. 4 shows the amperometric response of the graphene–AuNPs/GCE at −0.4 V upon successive adding H_2O_2 to a continuous stirring PBS solution. The inset of Fig. 4 shows the calibration curve based on reduction current responses in the presence of H_2O_2. The graphene–AuNPs/GCE had a good linear response to H_2O_2 in the range of 20–280 μM with a correlation coefficient of 0.997. The sensitivity of graphene–AuNPs/GCE was 3 μA μM^{-1} cm^{-1}, and the detection limit was estimated to be 6 μM at the signal-to-noise ratio of 3.

In addition, graphene–AuNPs/GCE also showed an excellent reduction towards O_2. Fig. 5 displays the electrocatalytic reduction of O_2 at bare/GCE, graphene/GCE, and graphene–AuNPs/GCE. An obvious reduction peak of O_2 was observed at ca. −0.45 V (green line) in O_2-saturated PBS solution. The reduced current at graphene–AuNPs/GCE indicated that graphene–AuNPs nanocomposites had much better electrocatalytic activity towards reduction of O_2 than other cases. From the comparison of the reduction of O_2 at bare/GCE and graphene/GCE, the peak current increased obviously, and the peak potential was more positive, which should be ascribed to the increase of active area of AuNPs when they were coupled on graphene nanosheets.

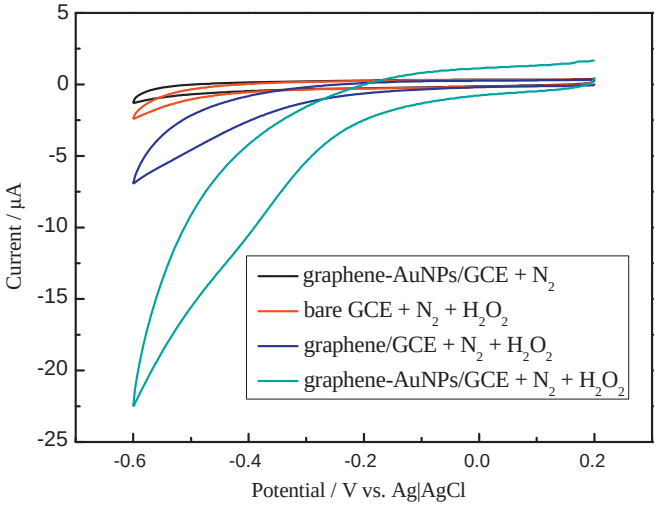

Fig. 3. Cyclic voltammograms of bare GCE (red), graphene/GCE (blue) and graphene–AuNPs/GCE (green) in 0.05 M N_2-saturated PBS solution (pH 7.4) in the presence of 0.05 M H_2O_2, and graphene–AuNPs/GCE (black) in N_2-saturated PBS solution (scan rate: 0.05 V s^{-1}). (For interpretation of the references to color in this figure legend, the reader is referred to the web version of this article.)

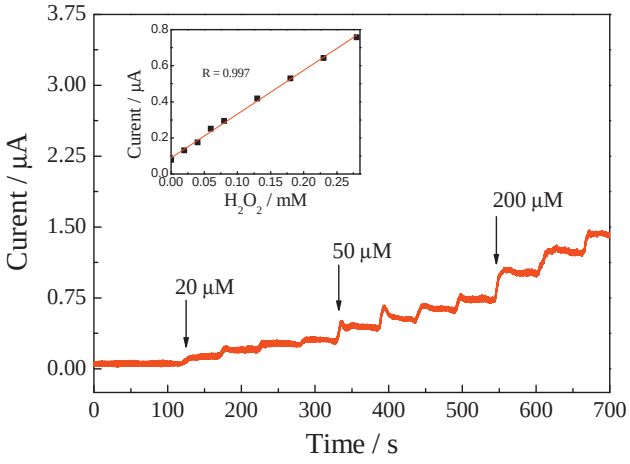

Fig. 4. Amperometric response of graphene–AuNPs/GCE electrode to H_2O_2 in N_2-saturated PBS solution at working potential of −0.4 V. Inset: calibration curve of H_2O_2 concentration on the modified electrode.

3.3. Interference study

As well known, some coexisted substances, such as glucose (Glc), uric acid (UA), dopamine (DA), ascorbic acid (AA), Ca^{2+}, Mg^{2+}

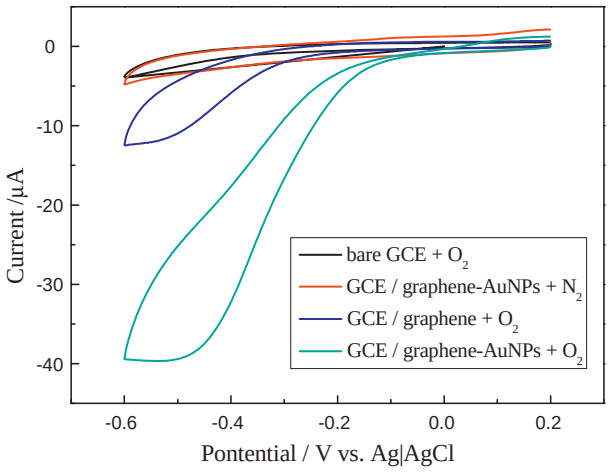

Fig. 5. Cyclic voltammograms at bare GCE (red), graphene/GCE (blue) and graphene–AuNPs/GCE (green) in 0.05 M PBS solution (pH 7.4) saturated with O_2, and graphene–AuNPs/GCE (black) in N_2-saturated PBS solution (scan rate: 0.05 V s^{-1}). (For interpretation of the references to color in this figure legend, the reader is referred to the web version of this article.)

and Cl^{1-} and so on, generally show the serious interference for electrochemical H_2O_2 detection, which limit the practical application of the sensor. Herein, in order to better detect the H_2O_2, we used the current–time (i–t) curve to evaluate the interference effect. As shown in Fig. S2, it was obvious that the current increased when 0.2 mM H_2O_2 was added to the PBS solution. However, when the interfering substances were injected into the PBS solution containing 0.2 mM H_2O_2, no significant interference could be observed for Glc, UA, DA, AA, Ca^{2+}, Mg^{2+} and Cl^-, indicating that these coexisting substances did not affect the determination of H_2O_2.

The river water samples were demonstrated for the applicability of the proposed biosensor for practical sample analysis. 50, 100 and 200 μM H_2O_2 solution were added into the river water samples, respectively. The average recovery of the biosensor was 92.2%, 94.6% and 104.3%, respectively, with the relative standard deviation (RSD) less than 4.6%. The rain water samples without adding H_2O_2 did not show any detectable signal.

3.4. Stability and reproducibility of the graphene–AuNPs/GCE

The stability of the graphene–AuNPs modified electrode was investigated using electrochemistry scan between −0.6 and 0.2 V in PBS solution. After storing in a refrigerator (4 °C) for 1 day, the response current was still retained at 98.1% of the initial response. After 7 and 15 days, 95.2% and 92.4% of its initial current were also obtained, respectively. This implied that the graphene–AuNPs nanocomposites film was very stable. What is more, the currents of 100 μM H_2O_2 solutions at five independent graphene–AuNPs/GCEs were recorded and the RSD value was calculated to be 3.4%, indicating the graphene–AuNPs nanocomposites film had reliable reproducibility.

4. Conclusions

In sum, a green, one-step method is proposed for the synthesis of graphene–AuNPs nanocomposites by introducing an environmentally friendly HMTA as reducing and stabilizing agent. The AuNPs demonstrate remarkably good dispersion and smaller size on graphene nanosheets. The resulting graphene–AuNPs nanocomposites show high electrocatalytic activity toward both O_2 and H_2O_2, due to the synergistic effect of graphene and AuNPs. The high electrocatalytic activity helps us with constructing a practical glucose biosensor in the next work.

Acknowledgements

The authors are most grateful to the NSFC (No. 20903082, 21105096 and 21175130), Chinese Academy of Sciences (No. KGCX2-YW-231, YZ200906 and YZ2010018) and Department of Science and Technology of Jilin Province (No. 201215091) for their financial support.

Appendix A. Supplementary data

Supplementary data associated with this article can be found, in the online version, at doi:10.1016/j.talanta.2012.02.050.

References

[1] A.K. Geim, K.S. Novoselov, Nat. Mater. 6 (2007) 183–191.
[2] C. Lee, X.D. Wei, J.W. Kysar, J. Hone, Science 321 (2008) 385–388.
[3] K.S. Novoselov, A.K. Geim, S.V. Morozov, D. Jiang, Y. Zhang, S.V. Dubonos, I.V. Grigorieva, A.A. Firsoy, Science 306 (2004) 666–669.
[4] A.K. Geim, Science 324 (2009) 1530–1534.
[5] H.K. He, C. Gao, Chem. Mater. 22 (2010) 5054–5064.
[6] S.H. Goh, M. Pumera, Anal. Chem. 82 (2010) 8367–8370.
[7] Y.X. Xu, H. Bai, G.W. Lu, C. Li, G.Q. Shi, J. Am. Chem. Soc. 130 (2008) 5856–5857.
[8] X.W. Liu, J.J. Mao, P.D. Liu, X.W. Wei, Carbon 49 (2011) 477–483.
[9] T.T. Baby, S.S.J. Aravind, T. Arockiadoss, R.B. Rakhi, S. Ramaprabhu, Sens. Actuators B 145 (2010) 71–77.
[10] J.M. Gong, X.J. Miao, T. Zhou, L.Z. Zhang, Talanta 85 (2011) 1344–1349.
[11] J.B. Liu, S.H. Fu, B. Yuan, Y.L. Li, Z.X. Deng, J. Am. Chem. Soc. 132 (2010) 7279–7281.
[12] F. Liu, J.Y. Choi, T.S. Seo, Chem. Commun. 46 (2010) 2844–2846.
[13] R. Muszynski, B. Seger, P.V. Kamat, J. Phys. Chem. C 112 (2008) 5263–5266.
[14] J. Han, Y. Zhuo, Y.Q. Chai, L. Mao, Y.L. Yuan, R. Yuan, Talanta 85 (2011) 130–135.
[15] Y.K. Kim, H.K. Na, D.H. Min, Langmuir 26 (2010) 13065–13070.
[16] D.H. Zhang, X.H. Liu, X. Wang, J. Inorg. Biochem. 105 (2011) 1181–1186.
[17] E.Y. Yoo, T. Okata, T. Akita, M. Kohyama, J. Nakamura, I. Honma, Nano Lett. 9 (2009) 2255–2259.
[18] R.S. Sundaram, C. Gomez-Navarro, K. Balasubramanian, M. Burghard, K. Kern, Adv. Mater. 20 (2008) 3050–3053.
[19] E. Katz, I. Willner, Angew. Chem. Int. Ed. 43 (2004) 6042–6108.
[20] X.D. Cao, Y.K. Ye, S.Q. Liu, Anal. Biochem. 417 (2011) 1–15.
[21] Y.G. Liu, X.M. Feng, J.M. Shen, J.J. Zhu, W.H. Hou, J. Phys. Chem. B 112 (2008) 9237–9242.
[22] T. Łuczak, Electrochim. Acta 54 (2009) 5863–5870.
[23] J.M. Pingarrón, P. Yóñez-Sedeño, A. González-Cortés, Electrochim. Acta 53 (2008) 5848–5866.
[24] J. Turkevich, P.C. Stevenson, J. Hillier, Discuss. Faraday Soc. 11 (1951) 55–75.
[25] M. Brust, M. Walker, D. Bethell, D.J. Schiffrin, R. Whyman, J. Chem. Soc., Chem. Commun. 7 (1994) 801–802.
[26] N.R. Jana, X. Peng, J. Am. Chem. Soc. 125 (2003) 14280–14281.
[27] M. Schulz-Dobrick, K.V. Sarathy, M. Jasen, J. Am. Chem. Soc. 127 (2005) 12816–12817.
[28] P.S. Kumar, A.S. More, R.D. Shingte, P.P. Wadgaonkar, M. Sastry, Adv. Mater. 16 (2004) 966–971.
[29] H. Hiramatsu, F.E. Osterloh, Chem. Mater. 16 (2004) 2509–2511.
[30] J.D.S. Newman, G.J. Blanchard, Langmuir 22 (2006) 5882–5887.
[31] A.M. Kirillov, Coord. Chem. Rev. 255 (2011) 1603–1622.
[32] S.B. Xu, Q. Yang, J. Phys. Chem. C 112 (2008) 13419–13425.
[33] D. Tian, G.P. Yong, Y. Dai, X.Y. Yan, S.M. Liu, Catal. Lett. 130 (2009) 211–216.
[34] K. Govender, D.S. Boyle, P.B. Kenway, P. O'Brien, J. Mater. Chem. 14 (2004) 2575–2591.
[35] X.P. Shen, L. Jiang, Z.Y. Ji, J.L. Wu, H. Zhou, G.X. Zhu, J. Colloid Interface Sci. 354 (2011) 493–497.
[36] W. Hummers, R. Offeman, J. Am. Chem. Soc. 80 (1958) 1339–1340.
[37] N.I. Kovtyukhova, P.J. Ollivier, B.R. Martin, T.E. Mallouk, S.A. Chizhid, E.V. Buzaneva, A.D. Gorchinskiy, Chem. Mater. 11 (1999) 771–778.
[38] T.F. Jaramillo, S.H. Baeck, B.R. Cuenya, E.W. McFarland, J. Am. Chem. Soc. 125 (2003) 7148–7149.